Freeze-out in hydrodynamical models

Cs. Anderlik,[1,2] L. P. Csernai,[1,2,3] F. Grassi,[4] W. Greiner,[2] Y. Hama,[4] T. Kodama,[5] Zs. I. Lázár,[1,2,6] V. K. Magas,[1] and H. Stöcker[2]

[1]*Section for Theoretical Physics, Department of Physics, University of Bergen, Allegaten 55, 5007 Bergen, Norway*
[2]*Institut für Theoretische Physik, Universität Frankfurt, Robert-Mayer-Strasse 8-10, D-60054 Frankfurt am Main, Germany*
[3]*KFKI Research Institute for Particle and Nuclear Physics, P.O. Box 49, 1525 Budapest, Hungary*
[4]*Instituto de Física, Universidade de Sao Paulo, CP 66318, 05389-970 São Paulo-SP, Brazil*
[5]*Instituto de Física, Universidade Federal do Rio de Janeiro, CP 68528, 21945-970 Rio de Janeiro-RJ, Brazil*
[6]*Department of Physics, Babeş-Bolyai University, Strada M. Kogălniceanu nr. 1, 3400 Cluj-Napoca, Romania*

We study the effects of strict conservation laws and the problem of negative contributions to final momentum distribution during the freeze-out through 3-dimensional hypersurfaces with spacelike normal. We study some suggested solutions for this problem, and demonstrate it in one example. [S0556-2813(99)04605-1]

I. INTRODUCTION

Fluid dynamical models, especially their simpler versions, are very popular in heavy ion physics, because they connect directly collective macroscopic matter properties, like the equation of state (EOS) or transport properties, to measurables.

Particles which leave the system and reach the detectors, can be taken into account via source (drain) terms in the 4-dimensional space-time based on kinetic considerations, or in a more simplified way via freeze-out (FO) or final break-up schemes, where the frozen out particles are formed on a 3-dimensional hypersurface in space-time. This information is then used as input to compute measurables such as two-particle correlation, transverse, longitudinal, radial, and cylindrical flow, transverse momentum and transverse mass spectra, etc.

In this paper we concentrate on freeze-out. A basic standard assumption in this case is that freeze-out happens across a hypersurface as already mentioned, so it can be pictured as a discontinuity where the kinetic properties of the matter, such as energy density and momentum distribution change suddenly. The hypersurface is an idealization of a layer of finite thickness (of the order of a mean free path or collision time) where the frozen-out particles are formed and the interactions in the matter become negligible. The dynamics of this layer is described in different kinetic models such as Monte Carlo models [1,2] or four-volume emission models [3–7]. In fact, the zero thickness limit of such a layer is an overidealization of kinetic freeze-out in heavy ion reactions, while it is applicable on more macroscopic scales like in astrophysics.[1]

Two types of hypersurfaces are distinguished: those with

___

[1]On the other hand, if kinetic freeze-out coincides with a rapid phase transition, like in the case of rapid deconfinement transition of supercooled quark-gluon plasma, the sharp freeze-out hypersurface idealization may still be applicable even for heavy ion reactions. It is, however, beyond the scope of this work to study the freeze-out dynamics and kinetics in this latter case.

a spacelike normal vector, $d\sigma^\mu d\sigma_\mu = -(d\sigma)^2$ (e.g., events happening on a propagating 2-dimensional surface) and those with a timelike normal vector $d\sigma^\mu d\sigma_\mu = (d\sigma)^2$ (a common example of which is an overall sudden change in a finite volume).

Once the freeze-out surface is determined, one can compute measurables. Landau, when drafting his hydrodynamical model [8], just evaluated the flow velocity distribution at freeze-out, and this distribution served as a basis for all observables. This approach was used in early fluid dynamical simulations of heavy ion collisions also [9–11]. This procedure was improved to add thermal velocities to the flow velocities at freeze-out, by Milekhin [12,13] and later by Cooper and Frye [14]. This method is widely used, however it raises at least three problems [15].

First, in some cases before the 1990s, the possible existence of discontinuities across hypersurfaces with timelike normal vectors was not taken into account or considered unphysical[2] [19–22]. This point was studied recently [23] so we do not discuss it further.

Second, since the kinetic properties of the matter are different on the two sides of the front, the explicit evaluation of conservation laws across the freeze-out surface should be taken into account which is not always easy to implement. In some (simple) cases [24–26], these conservation laws are enforced and discussed. For example in [24], it was pointed out that the freeze-out momentum distribution for hypersurfaces with timelike normal may become locally anisotropic.

___

[2]Taub [16] discussed discontinuities across propagating hypersurfaces, which have a spacelike normal vector. If one applies Taub's formalism from 1948, to freeze-out surfaces with timelike normal vectors, one gets a usual Taub adiabat but the equation of the Rayleigh line yields imaginary values for the particle current across the front. Thus, these hypersurfaces were thought unphysical. However more recently, Taub's approach has been generalized to these hypersurfaces [17] (see also [18]) while eliminating the imaginary particle currents arising from the equation of the Rayleigh line. Thus, it is possible to take into account conservation laws exactly across any surface of discontinuity with relativistic flow.

In [27] a solution for post FO massless, baryonfree Bose gas was presented. Here we recall the procedure that should be followed in Sec. II.

The *third* problem is a conceptual problem arising in the Cooper-Frye freeze-out description when we apply it to a hypersurface with spacelike normal: it is the problem of negative contributions (see Sec. II). This is the main subject of this paper. This problem appears in all freeze-out calculations up to now that we are aware of, and to our knowledge it was not satisfactorily discussed yet in the literature. It was recognized by some of those who applied the Cooper-Frye freeze-out description before [25,26,28]. A possible partial solution was presented in part 2 of Ref. [26] for noninteracting massless particles, in $1+1$ dimension using the post FO cut Jüttner ansatz. In [27] it was shown that in an oversimplified kinetic freeze-out model one can obtain the cut Jüttner distribution as post FO distribution. In Sec. IV we complete and generalize the results of [26] and present an example for the solution of the freeze-out problem. In Sec. V we suggest improvements that go beyond the cut Jüttner ansatz.

II. CONSERVATION LAWS ACROSS IDEALIZED FREEZE-OUT DISCONTINUITIES

In the zero width limit of the freeze-out domain (freeze-out surface), the energy-momentum tensor changes discontinuously across this surface. Consequently, the four-vector of the flow velocity may also change [17,29,30]. These changes should be discussed in terms of the conservation laws.

The invariant number of conserved particles (world lines) crossing a surface element, $d\sigma^\mu$, is

$$dN = N^\mu d\sigma_\mu, \tag{1}$$

and the total number of all the particles crossing the FO hypersurface, S, is

$$N = \int_S N^\mu d\sigma_\mu. \tag{2}$$

If we insert the kinetic definition of N^μ

$$N^\mu = \int \frac{d^3p}{p^0} p^\mu f_{FO}(x,p), \tag{3}$$

into Eq. (1) we obtain the Cooper-Frye formula [14]:

$$E\frac{dN}{d^3p} = \int f_{FO}(x,p)p^\mu d\sigma_\mu, \tag{4}$$

where $f_{FO}(x,p)$ is the post FO phase space distribution of frozen-out particles which is not known from the fluid dynamical model. The problem is to choose its form correctly. Usually one assumes that the pre FO momentum distribution as well as the post FO distribution are both local thermal equilibrium distributions, with the same temperature, boosted by the local collective flow velocity on the actual side of the freeze-out surface, although the post FO distribution need not be a thermal distribution. Parametrizing the post FO distribution as thermal, $f_{FO}(x,p;T,n,u^\mu)$, where T

does not necessarily coincide with the pre FO temperature, and knowing the pre FO baryon current and energy-momentum tensor, N_0^μ and $T_0^{\mu\nu}$, we can calculate the post freeze-out quantities N^μ and $T^{\mu\nu}$ from the relations [16,17]

$$[N^\mu d\sigma_\mu] = 0 \quad \text{and} \quad [T^{\mu\nu}d\sigma_\mu] = 0, \tag{5}$$

across a surface element[3] of normal vector $d\sigma^\mu$. Here $[A] \equiv A - A_0$. The post FO distribution is not a thermal equilibrium distribution, so temperature does not exist, nevertheless, the conservation laws fix the *parameters*, e.g., T, n,u^μ, of our momentum distribution, $f_{FO}(x,p;T,n,u^\nu)$.

To obtain a physically realizable result, in addition we have to check the condition for entropy increase:

$$[S^\mu d\sigma_\mu] \geq 0 \quad \text{or} \quad R = \frac{S^\mu d\sigma_\mu}{S_0^\mu d\sigma_\mu} \geq 1, \tag{6}$$

where, for both equilibrium and nonequilibrium FO distributions [18]

$$S^\mu = -\int \frac{d^3p}{p^0} p^\mu f_{FO}(x,p)[\ln\{(2\pi)^3 f_{FO}(x,p)\} - 1]. \tag{7}$$

This condition is not necessary to obtain a solution of the freeze-out problem, but it should always be checked to exclude nonphysical solutions. We have to note at this stage that the post FO distribution must not be an equilibrium (or stationary) solution of the Boltzmann transport equation, and consequently on the post FO side the energy flow, baryon flow, and entropy flow velocities may all be different.

We can now remind briefly what the problem of negative contributions to the Cooper-Frye formula is, and a possible way out. For a FO surface with timelike normal, both p^μ and $d\sigma^\mu$ are timelike vectors, thus,

$$p^\mu d\sigma_\mu > 0,$$

and the integrand in the integral (4) is always positive. For a FO surface with spacelike normal, p^μ is timelike and $d\sigma^\mu$ is spacelike, thus, $p^\mu d\sigma_\mu$ can be both positive and negative. (Note that p^μ may point now both in the post and pre FO directions.) Thus, the integrand in the integral (4) may change sign in the integration domain, and this indicates that part of the distribution contributes to a current going back, into the front while another part is coming out of the front. On the pre FO side p^μ is unrestricted and $p^\mu d\sigma_\mu$ may have both signs, because we are supposing that pre FO phase is in thermal equilibrium. However, in the zero width limit of the FO front, it is difficult to understand such a situation. What happens actually is that internal rescatterings occur inside the finite FO domain and feed particles back to the pre FO side to maintain the thermal equilibrium there. On the post FO side, however, we do not allow rescattering and back scattering any more. If a particle has passed the freeze-out do-

---

[3] In numerical calculations the local freeze-out surface can be determined most accurately via self-consistent iteration [26,31].

main it cannot scatter back. In other words, the post FO distribution should have the form [25,26],

$$f^*_{\text{FO}}(x,p,d\sigma^\mu)=f_{\text{FO}}(x,p)\Theta(p^\mu d\sigma_\mu), \qquad (8)$$

where $\Theta(x)$ is the step function. Consequently, this distribution cannot be an ideal gas distribution. (On the pre FO side, the distribution may or may not be ideal.) The conservation laws across a small element of the freeze-out front with spacelike normal take the form

$$\int_S \left(\int \frac{d^3p}{p^0} f^*_{\text{FO}}(x,p,d\sigma^\gamma)p^\mu \right) d\sigma_\mu = \int_S N_0^\mu(x)d\sigma_\mu, \qquad (9)$$

$$\int_S \left(\int \frac{d^3p}{p^0} f^*_{\text{FO}}(x,p,d\sigma^\gamma)p^\mu p^\nu \right) d\sigma_\mu$$

$$= \int_S T_0^{\mu\nu}(x)d\sigma_\mu. \qquad (10)$$

III. THE ALLOWED MOMENTUM REGION FOR SPACELIKE FO

Let us assume that the FO process happens in the positive x direction, in other words we go in the positive x direction from the pre FO domain to the post FO domain. The FO hypersurface has a spacelike normal $[d\sigma^\mu d\sigma_\mu = -(d\sigma)^2]$, so that $d\sigma_\mu$ is orthogonal to the hypersurface (i.e., to the timelike tangent vector of the surface t^μ, $t^\mu d\sigma_\mu = 0$) and points into the post FO (positive x) direction (while $d\sigma^\mu$ points in the pre FO direction).

Depending on the reference frame, the spacelike FO front can propagate both in the positive or negative x direction, or it can be Lorentz transformed into its own rest frame, the rest frame of the front (RFF), where $d\sigma_\mu = (0,1,0,0)d\sigma$. In other reference frames $d\sigma_\mu = \gamma(v,1,0,0)d\sigma$, where $\gamma = 1/\sqrt{1-v^2}$. The parameter $v = d\sigma_0/d\sigma_x = -t^x/t^0$ is frame dependent and may be both positive and negative.

In order to use the parameter v in the following discussion, we have to select a given reference frame and fix the value in that frame. Let us choose the frame *comoving with the peak* of the post FO invariant momentum distribution. Following Ref. [26] let us denote this frame as the rest frame of the gas (RFG). Note, however, that, contrary to what its name seems to suggest, this frame is *not the local rest frame* of the post FO matter, since the post FO distribution is not spherically symmetric in momentum space. Thus, for the following discussion we *define* v in the RFG frame as

$$v \equiv \left. \frac{d\sigma_0}{d\sigma_x} \right|_{\text{RFG}},$$

or we can also define and have the same v value, by using the velocity of the peak of the post FO distribution, u^μ_{RFG} in the RFF. (Note: this is not equal with the post FO flow velocities, neither with the Eckart, nor with the Landau flow velocity.) Thus,
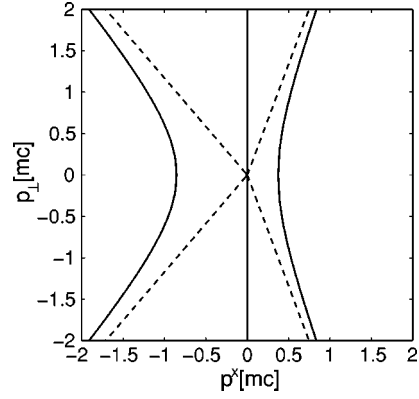

FIG. 1. The boundaries of the cut post FO distributions in the phase space indicating the regions where particles are allowed to freeze out. These boundaries are hyperboloids, for RFF velocities of $v=0.65$, $v=0$, and $v=-0.35$ (from left to right). Particles to the right of these hyperboloids may freeze out. While for large positive v values the cut is a small perturbation, for moderate or particularly for negative values of v the cut is far from negligible. The dashed lines show the massless limits.

$$v = \left. \frac{u^x_{\text{RFG}}}{u^0_{\text{RFG}}} \right|_{\text{RFF}},$$

and this means that in the RFF the peak four-velocity has the form $u^\mu_{\text{RFG}} = \gamma(1,v,0,0)|_{\text{RFF}}$. This velocity v can be both positive and negative in RFF, i.e., the peak velocity may point to the post FO direction (as we would expect), and also in the pre FO direction in RFF which seems to be confusing. This is, however, not a problem in itself because both flow velocities (Eckart and Landau) are always positive on the post FO side. As we will see later, in special cases it is possible that we obtain negative post FO peak velocity for positive pre FO flow velocities. This indicates we have to discuss the importance of the cut by $\Theta(p^\mu d\sigma_\mu)$, otherwise one might be tempted to believe that this cut is not affecting the post FO distribution too much, and the correct treatment causes only a few percent cut which is negligible. We show in the following that this is not the case.

The $p^\mu d\sigma_\mu > 0$ requirement in the RFG frame means that only momenta with component

$$p^x \geqslant -v \sqrt{m^2+(p^x)^2+(p_\perp)^2}, \qquad (11)$$

contribute to the post FO momentum distribution. This means that the boundaries of the allowed domain in the $[p^x, p_\perp]$ plane are hyperbolas in the post FO RFG

$$\frac{(p^x)^2}{\gamma^2-1} - (p_\perp)^2 = m^2, \qquad (12)$$

and the domains of the positive x side of the corresponding hyperboloids in the 3-dimensional momentum space may contribute to the FO distribution (Fig. 1). In the massless limit the hyperboloids become cones around the x axis and centered at the origin.

Dominant case. For $v=0$ the hyperboloid becomes a plane boundary at $p^x=0$ in RFG, i.e., the boundary cuts the Jüttner distribution in the middle (because in the RFG the

peak of the distribution is centered at $\vec{p}=0$). If $v>0$, the peak velocity points to the post FO direction and the cut hyperboloid is fully in the negative p^x region, thus for large v values only a smaller fraction is excluded from the full Jüttner distribution. Most of the particles described by a full Jüttner distribution freeze-out in this case. We will consider this as the dominant FO case.

On the other hand, as we can see in Fig. 1, for the $v<0$ case the peak flow points back into the pre FO direction, and only a small fraction of a full Jüttner distribution will freeze out. The cut eliminates the major part of the particles. This situation leads to less frozen-out particles, but it yields an unusual post FO distribution.

IV. CONSERVED CURRENTS FOR CUT JÜTTNER DISTRIBUTION

We now study the particular case where f_{FO} is a Jüttner (or relativistic Boltzmann [32,18]) distribution and so f_{FO}^* is a cut Jüttner distribution:

$$f_{FO}^*(p)=f^{Juttner}(p)\Theta(p^\mu d\sigma_\mu)$$

$$=\frac{\Theta(p^\mu d\sigma_\mu)}{(2\pi\hbar)^3}\exp\left(\frac{\mu-p_\mu u_{RFG}^\mu}{T}\right), \qquad (13)$$

where μ is the chemical potential related to the invariant scalar density $\hat{n}$, of the noncut Jüttner distribution as $\mu=T\ln[\hat{n}(2\pi\hbar)^3/(4\pi m^2 TK_2(m/T))]$, and u_{RFG}^μ, $\hat{n}$ and T are *parameters* of the distribution f_{FO}^* originating from the full Jüttner distribution. These are not the flow velocity, proper density, and temperature of the cut Jüttner distribution. The cut Jüttner distribution is not a thermal equilibrium distribution, e.g., it does not have a temperature at all.

This distribution for massless particles was considered in part 2 of Ref. [26] (also in [25]). The cut selects particles with momenta $p^\mu d\sigma_\mu>0$.

We can evaluate the baryon four-current, N^μ, by inserting the cut Jüttner distribution into the definition, Eq. (3), and we get a time directed, N^0, as well as a spatial component, N^x, (where x is the direction of the spatial component of the FO normal, $d\sigma^\mu$, in RFG). In Ref. [26] the spatial component, N^x, of the four-current was not evaluated, so seeing only the zeroth component, N^0, the unsuspecting reader might have believed falsely, that RFG (rest frame of the gas) is the local rest frame of the gas. Performing the calculation, in the post FO RFG frame the baryon current reads as

$$N^0=\frac{\tilde{n}}{4}\left\{vA+a^2j[(1+j)K_2(a)-\mathcal{K}_2(a,b)]+j\frac{b^3v^3}{3}e^{-b}\right\}$$

$$\overset{m=0}{\longrightarrow}\tilde{n}(\mu,T)\frac{v+1}{2}, \qquad (14)$$

$$N^x=\frac{\tilde{n}}{8}[(1-v^2)A-a^2e^{-b}]\overset{m=0}{\longrightarrow}\tilde{n}(\mu,T)\frac{1-v^2}{4},$$

where $j=\text{sign}(v)$, $\tilde{n}=8\pi T^3 e^{\mu/T}(2\pi\hbar)^{-3}$, $a=m/T$, so that $\hat{n}(\mu,T)=\tilde{n}a^2K_2(a)/2$ is the invariant scalar density of

the symmetric Jüttner gas, $b=a/\sqrt{1-v^2}$, $v=d\sigma_0/d\sigma_x$, $A=(2+2b+b^2)e^{-b}$, and

$$\mathcal{K}_n(z,w)\equiv\frac{2^n(n)!}{(2n)!}\;z^{-n}\int_w^\infty dx\;(x^2-z^2)^{n-1/2}\;e^{-x},$$

i.e., $\mathcal{K}_n(z,z)=K_n(z)$. Just as in case of the noncut distributions the cut Jüttner distribution yields few modified Bessel functions in the expression of the four-currents, while the relativistic Fermi and relativistic Bose distributions lead to a series of these functions. When evaluating the limits we used the relation $\mathcal{K}_n(a,b)\overset{a=b}{\rightarrow}K_n(a)\overset{a=0}{\rightarrow}2^{n-1}(n-1)!a^{-n}$. This baryon current may then be Lorentz transformed into the Eckart local rest (ELR) frame of the post FO matter, which moves with $u_E^\mu=N^\mu/(N^\nu N_\nu)^{1/2}=\gamma_E(1,v_E,0,0)|_{RFG}$ in the RFG, or alternatively into the rest frame of the freeze-out front (RFF), where $d\sigma_\mu=(0,1,0,0)d\sigma$ and the velocity of the RFG is $u_{E,RFG}^\mu=\gamma(1,v,0,0)|_{RFF}$. Then the Eckart flow velocity of the matter represented by the cut Jüttner distribution viewed from the RFF is $u_E^\mu=\gamma_c(1,v_c,0,0)|_{RFF}$, where $v_c=(v+v_E)/(1+vv_E)$.

The proper density (i.e., the density in the ELR frame) is obtained as

$$n(\mu,T,v)=\sqrt{N^\nu N_\nu}. \qquad (15)$$

Note that the proper density of the cut Jüttner distribution, n, is reduced compared to the proper density of the complete spherical Jüttner distribution, $\hat{n}$.

The energy momentum tensor in the post FO RFG is

$$T^{00}=\frac{3\tilde{n}T}{2}\left\{\frac{ja^2}{2}\left\{(1+j)\left[K_2(a)+\frac{a}{3}K_1(a)\right]\right.\right.$$

$$\left.\left.-\left[\mathcal{K}_2(a,b)+\frac{a}{3}\mathcal{K}_1(a,b)\right]\right\}+Bv\right\},$$

$$T^{0x}=\frac{3\tilde{n}T}{4}\left\{(1-v^2)B-\frac{a^2}{6}(b+1)e^{-b}\right\},$$

$$T^{xx}=\frac{\tilde{n}T}{2}\left\{j\frac{a^2}{2}[(1+j)K_2(a)-\mathcal{K}_2(a,b)]+v^3B\right\},$$

$$T^{yy}=\frac{3\tilde{n}T}{4}\left\{v\left(1-\frac{v^2}{3}\right)B+\frac{ja^2}{3}[(1+j)K_2(a)-\mathcal{K}_2(a,b)]\right.$$

$$\left.-\frac{va^2}{6}(b+1)e^{-b}\right\}, \qquad (16)$$

where $B=(1+b+b^2/2+b^3/6)e^{-b}$ and $T^{zz}=T^{yy}$. This energy-momentum tensor may then be Lorentz transformed into the Landau local rest (LLR) frame of the post FO matter, which moves with u_L^μ in the RFG, or into the rest frame of the freeze-out front (RFF) where $d\sigma^\mu=(0,1,0,0)d\sigma$. Alternatively both flow velocities, μ_L^μ or μ_E^μ, can be transformed to the frame where we want to evaluate the conservation laws, Eq. (5), and the parameters of the post FO, cut

Jüttner distribution can be determined so that they satisfy the conservation laws. In the massless limit the energy momentum tensor in the RFG is

$$T^{00} = 3\tilde{n}T(v+1)/2, \quad T^{0x} = 3\tilde{n}T(1-v^2)/4,$$

$$T^{xx} = \tilde{n}T(v^3+1)/2, \quad T^{zz} = T^{yy} = (T^{00} - T^{xx})/2.$$

In addition we have to check the entropy condition. In the RFG frame the entropy current reads

$$S^0 = \frac{\tilde{n}}{4}\left\{\left(1-\frac{\mu}{T}\right)vA + 6vB + \left(1-\frac{\mu}{T}\right)a^2 j[(1+j)K_2(a)\right.$$

$$\left. - \mathcal{K}_2(a,b)] + ja^2[(1+j)K_1(a) - \mathcal{K}_1(a,b)]\right\}$$

$$\overset{m=0}{\rightarrow} \frac{\tilde{n}(\mu,T)}{2}(v+1)\left(4-\frac{\mu}{T}\right),$$

$$S^x = \frac{\tilde{n}}{8}\left[(1-v^2)\left(1-\frac{\mu}{T}\right)A + 6(1-v^2)B - a^2\right.$$

$$\left. \times \left(2+b-\frac{\mu}{T}\right)e^{-b}\right]$$

$$\overset{m=0}{\rightarrow} \frac{\tilde{n}(\mu,T)}{4}(1-v^2)\left(4-\frac{\mu}{T}\right). \quad (17)$$

Note that in the $m=0$ limit the vectors S^μ and N^μ are parallel to each other. This is explained by Fig. 1, which shows that in the RFG the cut in the $m=0$ limit becomes a central cone, and since the distribution is centrally symmetric in this frame, the integrals will be proportional to each other.

Solubility of the freeze-out problem

The situation is nontrivial and we have to take into account the possible directions of the flow and of $d\sigma_\mu$. Note: we must not assume that the flow is parallel to the freeze-out direction.

Let us start on the pre FO side labeled by "0." Here in the LR frame $u_0^\mu = (1,0,0,0)|$ and we can choose the x direction in this frame to point into the FO direction, so that $d\sigma_\mu = \gamma_0(v_0,1,0,0)d\sigma$. We assume that we know the FO hypersurface, i.e., we know v_0. Then, in this frame the conservation laws have three nonvanishing components yielding three known parameters $N_0^\mu d\sigma_\mu$, $T_0^{0\mu}d\sigma_\mu$, and $T_0^{x\mu}d\sigma_\mu$.

To find the solution we need these values in the RFG frame. However, the 3-dimensional direction of the x axis will not change because the front is assumed to be isotropic in its own $[y,z]$-plane. Thus, in the RFG the peak flow parameter is $u_{RFG}^\mu = (1,0,0,0)|_{RFG}$, and the normal of the FO front is $n_\mu = \gamma(v,1,0,0)$. Note that $v \neq v_0$. Furthermore, let us recall that the parameter v determines the post FO peak flow parameter in RFF, $u_{RFG}^\mu = \gamma(1,v,0,0)|_{RFF}$ (where $d\sigma_\mu = (0,1,0,0)d\sigma|_{RFF}$).

Consequently the conservation laws (9),(10) yield three nonvanishing equations in the RFG frame,

$$[N^\mu d\sigma_\mu] = 0, \quad [T^{0\mu}d\sigma_\mu] = 0 \quad \text{and} \quad [T^{x\mu}d\sigma_\mu] = 0,$$

which can determine the three unknown *parameters* of the post FO cut Jüttner distribution, v, T, and n (or μ). While the first equation is an invariant scalar, the remaining two are components of a 4-vector, so they should be transformed into the same reference frame, i.e., to RFG. Since we evaluated the quantities based on the cut Jüttner distribution in the RFG, we also need the pre FO quantities in the RFG. These can be determined by using the standard fluid dynamical form of $T^{\mu\nu}$ as seen from the RFG. From this frame the pre FO flow velocity is given by the difference of the pre and post FO flow velocities: $u_0^\mu = \gamma_{0R}(1,v_{0R},0,0)|_{RFG}$, where $v_{0R} = (v_0-v)/(1-v_0 v)$.

In the general case the solution can be obtained numerically. In the $m=0$ limit the solution is simpler and gives an interesting insight into the problem. The continuity equation leads to the equation

$$Q^{-2}(v+1)^3 + v - 1 = 0, \quad (18)$$

where $Q^{-1} = Q_1^{-1}(\mu,T) = \tilde{n}(\mu,T)/(4n_0\gamma_0 v_0)$, which leads to a third order equation and can be solved for v analytically. The energy equation, $[T^{0\mu}d\sigma_\mu] = 0$, leads to the same equation but with another coefficient $Q^{-1} = Q_2^{-1}(\mu,T) = 3T\tilde{n}(\mu,T)/(4e_0\gamma_0 v_0)$, thus, these two equations can have one and the same solution for v, only if the two coefficients, Q_1 and Q_2, are equal, which results in

$$T = \frac{1}{3}\frac{e_0}{n_0},$$

and the solutions of both third order equations yield the same expression:

$$v = v_{3rd}(\mu) = Q^{2/3}\{[1+\sqrt{1+Q^2/27}]^{1/3}$$

$$+ [1-\sqrt{1+Q^2/27}]^{1/3}\} - 1. \quad (19)$$

Then, dividing the equation $[T^{0\mu}d\sigma_\mu] = 0$, by the equation $[T^{x\mu}d\sigma_\mu] = 0$, yields another third order equation for v:

$$R_0 v^3 + 3v^2 + 3(2-R_0)v + 3 - 2R_0 = 0,$$

where $R_0 = e_0 v_0/p_0$. This equation can be solved analytically and yields one physical root, $v = 2 - 3/R_0$ (and two unphysical ones $v = -1$). Inserting v then into Eq. (18), we can obtain the resulting chemical potential, μ, also.

The possibility of this simple analytic solution is a consequence of the fact that in the $m=0$ limit the cut of the Jüttner distribution is made along central cones in the RFG, which then divide the energy and the baryon charge exactly in the same proportions.

As an illustration we studied the freeze-out of quark-gluon plasma (QGP) to cut Jüttner gas, in the massless limit. The pre FO side QGP is described by the most simple bag-model EOS [Eqs. (5.28)–(33) in Ref. [18]], thus local equilibrium is assumed and all pre FO parameters are assumed to be known including the baryon, energy-momentum and entropy currents.

On the post FO side these currents were evaluated earlier in this section, and the equations arising from the conservation laws, Eq. (5), were solved as presented above. Figure 2 indicates the change of flow velocity during freeze-out.
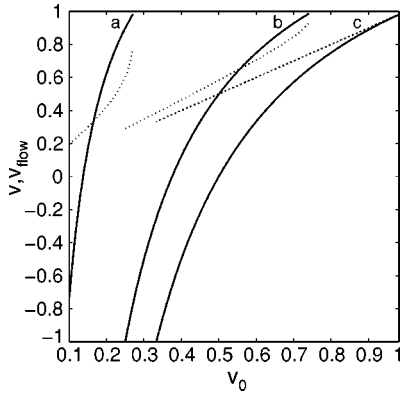
FIG. 2. Change of velocities in freeze-out of QGP to hadronic matter described by massless cut Jüttner distribution. The final velocity *parameters* (full lines) of the cut Jüttner distribution are plotted versus the initial flow velocity of QGP measured in the rest frame of the front (RFF) for case: (a) $n_0 = 1.2$ fm^{-3}, $T_0 = 60$ MeV, $\Lambda_B = 225$ MeV, (b) $n_0 = 0.1$ fm^{-3}, $T_0 = 60$ MeV, $\Lambda_B = 80$ MeV, and (c) $n_0 = 1.2$ fm^{-3}, $T_0 = 60$ MeV, $\Lambda_B = 0$ MeV. Observe that for small initial flow velocities the center of the cut Jüttner distribution moves backwards, although all the particles which are allowed to freeze out move forward. Thus, the post FO *baryon flow velocities* (dotted lines) are positive. Note the large acceleration caused by the released latent heat in cases (a) and (b). $\Lambda_B = B^{1/4}$, where B is the bag constant.

Physical solution exists only for positive initial velocities, $v_0 \geq 0$. The velocity *parameter* of the post FO cut Jüttner distribution varies from -1 to $+1$, but the post FO Eckart flow velocity is of course always positive in RFF. Thus, the post FO baryon current is also positive in RFF (this is obvious since we do not allow any particle to cross the front backwards), and consequently, the pre FO current and v_0 should also be positive because of the continuity equation. For small initial velocities, $v_0 \to 0$, the post FO velocities approach zero also, but for moderate velocities, deduced recently from experiments, $v = 0.3 - 0.7$, the difference between the post and pre FO flow velocities may be essential.

In order to show the effect of these modifications compared to the original Cooper-Frye treatment (where the increase of the flow velocity is ignored) we can consider case (a) in Fig 2. The cut Jüttner distribution always leads to an exponential p_t spectrum, but according to the new modified treatment starting from $v_0 = 0.2$ the post FO flow velocity increases to $v_{\text{flow}} = 0.4$, while the post FO parameter velocity (which determines the p_t spectrum) increases to $v = 0.6$. This corresponds to an increase of the slope parameter, T_{slope}, by 60%. This is due to the large latent heat arising from the large value of the bag constant taken in case (a). In case (b) the same effect is present but it is weaker. This change of the flow velocity is a basic feature of the correct freeze-out treatment, and it is a consequence of the conservation laws and not of the positivity requirement of $p^\mu d\sigma_\mu$ in spacelike FO. Thus, the flow velocity change occurs both in spacelike and in timelike freeze-out. This effect can cause for example the conversion of latent heat to collective kinetic energy and not to heat if the freeze-out coincides with an exotherm phase transition [29].

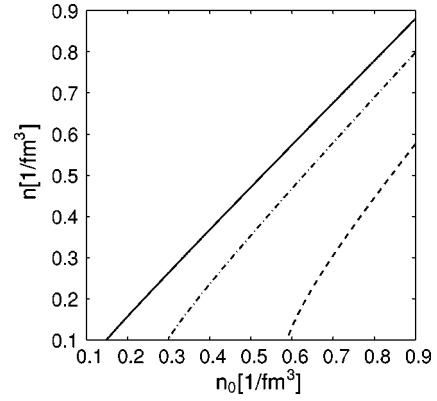Figure 3 shows that the baryon density, Eq. (15), decreases in the freeze-out process. This is connected to the

FIG. 3. The final baryon density, n, as a function of the pre FO baryon density. The baryon density decreases in the freeze-out process for cases $v_0 = 0.5$, $T_0 = 50$ MeV, (a) $\Lambda_B = 80$ MeV (full line), (b) $\Lambda_B = 120$ MeV (dashed-dotted line), and (c) $\Lambda_B = 160$ MeV (dashed line).

fact that the post FO flow velocities are above the pre FO ones, as shown in Fig. 2.

We should mention that the post FO temperature *parameter* of the cut Jüttner distribution becomes rather high, about an order of magnitude higher than the pre FO temperature. However, we have to recall that the term temperature is not applicable for a nonequilibrium distribution, therefore this result has no physical significance, it just illustrates the parametrization of the distribution of the assumed cut Jüttner shape.

Finally we have to check the entropy condition for these solutions. As we know [29,20,33] QGP can freeze out to hadronic matter with entropy production only if the QGP is supercooled or considerably supercooled. This remains valid for the cut Jüttner assumption as post FO distribution also. With most parametrizations only low temperature QGP is able to freeze-out. For the cut Jüttner gas we cannot speak of a critical temperature, because this gas is not in equilibrium and consequently cannot be in phase equilibrium either. Still this distribution can be attributed an entropy current by its kinetic definition, and the entropy condition can be checked (Fig. 4).

In reality the entropy condition is not so stringent as Fig. 4 indicates. In this illustrative study the post FO EOS had relatively few degrees of freedom to accomodate the high entropy content of QGP. By including many post FO mesons and other hadronic degrees of freedom in our post FO EOS, the entropy condition can be satisfied in a much wider range of parameters.

V. FREEZE-OUT DISTRIBUTION FROM KINETIC THEORY

We have seen that taking the cut Jüttner distribution as an ansatz for the post FO distribution, we can solve the freeze-out problem formally. Although we can satisfy all requirements, the obtained parameter values make it questionable whether the cut Jüttner ansatz is an adequate assumption. The shape of the distribution with the sharp cuts is also a rather unphysical feature of the distribution.

To obtain more realistic, and physically better applicable FO distributions, we should evaluate the distribution in more
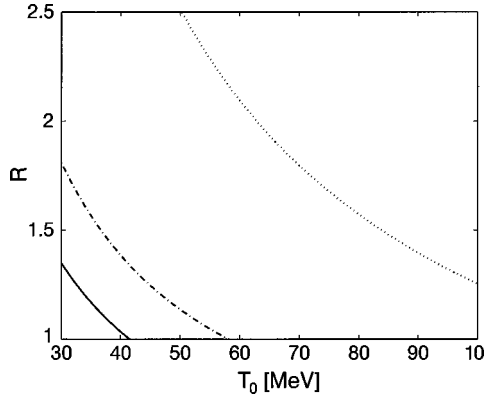
FIG. 4. The ratio of post FO and pre FO entropy currents transverse to the freeze-out front. Freeze-out can be physically realized if $R > 1$. The entropy condition is tested for three cases: (a) $n_0 = 0.1$ fm^{-3}, $v_0 = 0.5$, $\Lambda_B = 80$ MeV (full line), (b) $n_0 = 0.5$ fm^{-3}, $v_0 = 0.5$, $\Lambda_B = 80$ MeV (dashed line), and (c) $n_0 = 1.2$ fm^{-3}, $v_0 = 0.5$, $\Lambda_B = 225$ MeV (dotted line).

physical, microscopic nonequilibrium models. Kinetic theory is a straightforward candidate for this task.

A first very simplified attempt to solve the freeze-out problem dynamically in one dimensional kinetic model [27] returned the cut Jüttner distribution also, but only in highly unrealistic situations: only when the model yielded incomplete freeze-out. Thus, further work is needed to find physically realistic post freeze-out distributions in kinetic models or in other dynamical microscopic models.

VI. CONCLUSIONS

The importance of taking into account conservation laws in the description of the freeze-out process is pointed out. For freeze-out across hypersurfaces with spacelike normals the approach suggested by Bugaev [26], assuming cut Jüttner distribution as post freeze-out distribution is worked out, and the freeze-out problem was solved as an example for QGP freezing out into a cut Jüttner gas. This calculation indicates that results including the Cooper-Frye freeze-out procedure should be reconsidered and new emphasis should be given to the precise evaluation of the post freeze-out particle distributions.

The deviation from the earlier Cooper-Fry approach (where changes of flow velocity, density, and temperature were ignored) is apparent if the pre FO matter has large energy content in the form of compressional energy, latent heat, or in any other way, which is not present in the post FO, noninteracting matter. As this post FO matter is not necessarily in thermal equilibrium, we cannot consider it as a thermal phase with equilibrium thermodynamical parameters. Thus, this idealized approach assuming a FO surface is always assuming a discontinuity irrespective of what was the phase of the pre FO matter. Nevertheless, this treatment leads to the strongest modifications in cases when a first order phase transition with large latent heat is coupled to the freeze-out process.

Here we have considered an idealized transition as a discontinuity across a hypersurface. In as much as the flow across the surface is stationary our results are valid irrespective of the surface thickness, because we used only conservation laws. On the other hand in heavy ion reactions the flow across the surface can be considered stationary only if it is 1–2 fm wide. With purely kinetic freeze-out this is not a very realistic assumption [1]. On the other hand rapid hadronization from supercooled QGP may satisfy the required conditions and the sharp surface approximation is then realistic [34].

[1] L.V. Bravina, I.N. Mishustin, N.S. Amelin, J.P. Bondorf, and L.P. Csernai, Phys. Lett. B **354**, 196 (1995).

[2] L.V. Bravina, I.N. Mishustin, J.P. Bondorf, and L.P. Csernai, Heavy Ion Phys. **5**, 455 (1997).

[3] H.W. Barz, L.P. Csernai, and W. Greiner, Phys. Rev. C **26**, 740 (1982).

[4] F. Grassi, Y. Hama, and T. Kodama, Phys. Lett. B **355**, 9 (1995).

[5] F. Grassi, Y. Hama, and T. Kodama, Z. Phys. C **73**, 153 (1996).

[6] F. Grassi, Y. Hama, T. Kodama, and O. Socolowski, Heavy Ion Phys. **5**, 417 (1997).

[7] H. Heiselberg, Heavy Ion Phys. **5**, 435 (1997).

[8] L.D. Landau, Izv. Akad. Nauk SSSR, Ser. Fiz. **17**, 51 (1953).

[9] W. Scheid, H. Müller, and W. Greiner, Phys. Rev. Lett. **13**, 741 (1974).

[10] A.A. Amsden, G.F. Bertsch, F.H. Harlow, and J.R. Nix, Phys. Rev. Lett. **35**, 905 (1975); A.A. Amsden, F.H. Harlow, and J.R. Nix, Phys. Rev. C **15**, 2059 (1977).

[11] A.A. Amsden, A.S. Goldhaber, F.H. Harlow, and J.R. Nix, Phys. Rev. C **17**, 2080 (1978).

[12] G. Milekhin, Zh. Eksp. Teor. Fiz. **35**, 1185 (1958) [Sov. Phys. JETP **35**, 829 (1959)].

[13] G.A. Milekhin, Trudy FIAN **16**, 51 (1961).

[14] F. Cooper and G. Frye, Phys. Rev. D **10**, 186 (1974).

[15] L.P. Csernai, Zs.I. Lázár, and D. Molnár, Heavy Ion Phys. **5**, 467 (1997).

[16] A.H. Taub, Phys. Rev. **74**, 328 (1948).

[17] L.P. Csernai, Zh. Eksp. Teor. Fiz. **92**, 379 (1987) [Sov. Phys. JETP **65**, 216 (1987)].

[18] L.P. Csernai, *Introduction to Relativistic Heavy Ion Collisions* (Wiley, New York, 1994).

[19] M. Gyulassy, K. Kajantie, H. Kurki-Suonio, and L. McLerran, Nucl. Phys. **B237**, 477 (1984).

[20] P. Danielewicz and P.V. Ruuskanen, Phys. Rev. D **35**, 344 (1987).

[21] B.H. Liu, L. McLerran, and N. Turok, Phys. Rev. D **46**, 2668 (1992).

[22] N. Bilic, J. Cleymans, E. Suhonen, and D.W. von Oertzen, Phys. Lett. B **311**, 266 (1993).

[23] M.I. Gorenstein, H.G. Miller, R.M. Quick, and R.A. Ritchie, Phys. Lett. B **340**, 109 (1994).

[24] M.I. Gorenstein and Yu.M. Sinyukov, Phys. Lett. **142B**, 425 (1984).

[25] Yu.M. Sinyukov, Yad. Fiz. **50**, 228 (1989) [Sov. J. Nucl. Phys. **50**, 143 (1989)]; Z. Phys. C **43**, 401 (1989).

[26] K.A. Bugaev, Nucl. Phys. **A606**, 559 (1996).

[27] C. Anderlik, Z.I. Lázár, V.K. Magas, L.P. Csernai, H. Stöcker, and W. Greiner, Phys. Rev. C **59**, 369 (1999).

[28] S. Bernard, J.A. Maruhn, W. Greiner, and D.H. Rischke, Nucl. Phys. **A605**, 566 (1996).

[29] T. Csörgő and L.P. Csernai, Phys. Lett. B **333**, 494 (1994).

[30] L.P. Csernai and M. Gong, Phys. Rev. D **37**, 3231 (1988).

[31] J.J. Neumann, B. Lavrenchuk, and G. Fai, Heavy Ion Phys. **5**, 27 (1997).

[32] F. Jüttner, Ann. Phys. Chemie **34**, 865 (1911).

[33] L.P. Csernai and J.I. Kapusta, Phys. Rev. Lett. **69**, 737 (1992).

[34] L.P. Csernai and I.N. Mishustin, Phys. Rev. Lett. **74**, 5005 (1995).